N. Hansen, T. Bierkandt, N. Gaiser, P. Oßwald, M. Köhler, P. Hemberger, Formation of five-membered ring structures via reactions of *o*-benzyne, Proc. Combust. Inst. 40 (2024) 105623.

The original publication is available at www.elsevier.com

https://doi.org/10.1016/j.proci.2024.105623

Formation of five-membered ring structures via reactions of *o*-benzyne

Nils Hansen[a,*], Thomas Bierkandt[b], Nina Gaiser[b], Patrick Oßwald[b], Markus Köhler[b], Patrick Hemberger[c]

[a]*Combustion Research Facility, Sandia National Laboratories, Livermore, CA 94550, USA*
[b]*German Aerospace Center (DLR), Institute of Combustion Technology, 70569 Stuttgart, Germany*
[c]*Laboratory for Synchrotron Radiation and Femtochemistry, Paul Scherrer Institut (PSI), CH-5232 Villigen, Switzerland*

Abstract

The formation of five-membered ring structures is important for the generation of curved and bowl-shaped polycyclic aromatic hydrocarbons (PAHs) under combustion conditions. Here, we report the identification of the indenyl (C_9H_7) radical – the simplest aromatic hydrocarbon radical carrying an adjacent five- and six-membered ring, as the major product of the *o*-benzyne (*o*-C_6H_4) reaction with propargyl (C_3H_3). Because real flames exhibit a complex chemistry, elucidation of a specific reaction is very challenging. Instead, we studied the *o*-C_6H_4 + C_3H_3 reaction in a resistively heated microtubular SiC reactor at controlled conditions of 1150 K and a pressure near 10-20 Torr. To this end, the reactants *o*-benzyne and propargyl were pyrolytically generated from benzoyl chloride and propargyl bromide. We identified the reactants and the indenyl radical isomer-selectively utilizing photoion mass-selected threshold photoelectron spectroscopy (ms-TPES). The experimentally observed predominant formation of indenyl radicals finally confirms the theoretical predictions of Matsugi and Miyoshi [Phys. Chem. Chem. Phys. 14 (2012), 9722-9728] and highlights a versatile route for the formation of five-membered rings and curved PAHs via reactions of *o*-benzyne that favor the formation of multiring species over aliphatically substituted aromatic species.

Keywords: polycyclic aromatic hydrocarbons (PAHs); molecular-weight growth; propargyl; *o*-benyzne; threshold photoelectron spectroscopy (TPES)

---

*Corresponding author: nhansen@sandia.gov

Information for Colloquium Chairs and Cochairs, Editors, and Reviewers

1) Novelty and Significance Statement

The novelty of this research is manifold. A) Understanding the formation of five-membered ring structures in combustion environments is important for our understanding of the formation of curved and bowl-shaped PAHs. B) We provide clear evidence that reactions of *o*-benzyne provide versatile routes to five-membered ring-structures. C) The application of advanced analytic techniques such as mass-selected threshold photoelectron spectroscopy. Specifically, we used photoelectron-photoion coincidence spectroscopy (PEPICO) with single-energy vacuum-ultraviolet (VUV) radiation from the Swiss Light Source.

2) Author Contributions

- NH, TB, NG, PO, MK, and PH co-designed the study and executed the experiments. All authors participated in the analysis of the data and the editing and revision of the manuscript.

3) Authors' Preference and Justification for Mode of Presentation at the Symposium

The authors prefer **OPP** presentation at the Symposium, for the following reasons:

- This work provides an unambiguous identification of the reaction product of the *o*-benzyne reaction with propargyl radicals.
- This work is important for our understanding of molecular reaction mechanisms leading to molecular-weight growth and formation of polycyclic aromatic hydrocarbons.
- This reaction presents a versatile route to the formation of five-membered ring structures, i.e., indenyl, which are essential for the formation of curved PAHs.
- The results can be included in reaction mechanisms and can even be generalized for other reactions, thus providing a pathway to assembling a comprehensive PAH formation mechanism.

1. Introduction

Polycyclic aromatic hydrocarbons (PAHs) and soot, which are undesirable byproducts of incomplete combustion processes, are hazardous to the environment and pose a risk to human health [1-5]. The role of PAHs as soot precursors on the environment has recently gained renewed interest in the aviation sector because a major contribution to aviation's climate impact is attributed to soot induced contrail formation [6, 7]. Previous studies have shown a direct relation of ice nucleation and engine particle emission as well as the steering possibility via smart design of fuel composition [8-10].

The transition to clean and climate-neutral combustion technologies requires a comprehensive chemical understanding of the kinetics and mechanism of PAH and soot formation processes. Here, we provide information about the origins and reaction pathways leading to five-membered aromatic ring structures.

Such five-membered ring structures are the fundamental building blocks of non-planar polycyclic aromatic hydrocarbons (PAHs) and are crucial for soot formation in combustion environments [5]. Indene (C_9H_8), and the resonance-stabilized indenyl (C_9H_7) radical, are the simplest closed-shell and radical species that consist of a fused six- and five-membered rings (Scheme 1).

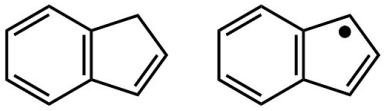

Scheme 1. Molecular structures of indene and indenyl.

Insights into the formation of these simple, prototypical aromatic structures is crucial to discover new formation pathways of larger five-membered ring structures. Furthermore, understanding the reactivity of five-membered rings aids the development of a chemical description of molecular-weight growth and soot formation processes.

Many indene formation pathways have been proposed and tested in comprehensive combustion chemistry mechanisms [11]. These reactions include, but are not limited to, reactions of phenyl (C_6H_5) radicals with propargyl (C_3H_3), allene/propyne (C_3H_4), allyl (C_3H_5), and propene (C_3H_6) [12-19]. In most comprehensive combustion chemistry mechanisms, indenyl is formed from H-abstraction of the closed-shell indene, but other channels are likely to be important as well.

For example, Matsugi and Miyoshi suggested that the reactions of *o*-benzyne (*o*-C_6H_4) with propargyl (C_3H_3) and benzyl (C_7H_7) are also versatile routes for the formation of five-membered ring structures, leading to indenyl and fluorenyl radicals [20]:

$$o\text{-}C_6H_4 + C_3H_3 \rightleftarrows C_9H_7 \quad \text{(R1)}$$

$$o\text{-}C_6H_4 + C_7H_7 \rightleftarrows \ldots \rightleftarrows C_{13}H_9 + H + H \quad \text{(R2)}$$

o-benzyne is an aromatic molecule with one more π-bond than benzene. Because of the ring-structure, it is not possible to have a linear C-C≡C-C bond and consequently an angle strain makes benzyne a highly reactive species. Although *o*-C_6H_4 is best described as a strained alkyne, it possesses non-negligible biradical character that impacts its reactivity [21, 22].

In combustion environments, *o*-C_6H_4 is mainly formed through thermal decomposition of phenyl (C_6H_5) radicals [23], and its reactions have been recognized to be important for the formation of large aromatic species in combustion environments [24-27]. It is conceivable that reactions of *o*-benzyne and resonance-stabilized radicals (RSRs) - not just propargyl (C_3H_3), but also allyl (C_3H_5), cyclopentadienyl (C_5H_5) and others - may significantly contribute to PAH formation. Such RSRs have been identified as important precursors in PAH and soot formation [4, 5, 28]. They exhibit longer lifetimes and larger concentrations in combustion environments due to their enhanced stability through the delocalization of the unpaired electron.

In previous work, McCabe *et al.* showed through a combination of experimental and theoretical work that indene (C_9H_8) + H is the primary product channel of the *o*-C_6H_4 + allyl (C_3H_5) reaction [29]. Comandini and Brezinsky showed theoretically that the reaction of *o*-C_6H_4 with cyclopentadienyl (C_5H_5) at higher temperatures can lead to the formation of indenyl (C_9H_7) + acetylene (C_2H_2) [30].

Given the dominance and importance of the propargyl (C_3H_3) radical in the formation of polycyclic aromatic hydrocarbons, it is surprising that information on the reactivity of propargyl with *o*-benzyne is scarce. Although it is well documented that propargyl is important for the formation of benzene, indene, naphthalene, and other aromatic species, [4, 5, 11, 31-33], including aliphatically substituted PAHs [18, 33], studies of reaction (R1) so far have remained theoretical [20].

According to this earlier theoretical work [20], reaction (R1) proceeds via the two initial adducts C_6H_4-CH_2-C≡CH and C_6H_4-CH=C=CH_2 that are formed through association with the CH_2-side (head) and CH-side (tail) of the propargyl radical. Subsequently, these intermediates can undergo ring closure to a cyclopentenyl-fused benzene that isomerizes without a substantial barrier to indenyl, the most stable C_9H_7 radical (see Scheme 2).

In this work, we performed experimental research to complement the earlier theoretical work of reaction (R1). We used a microtubular flash pyrolysis reactor to generate the reactants in a clean fashion and at sufficiently high number densities. Using photoion

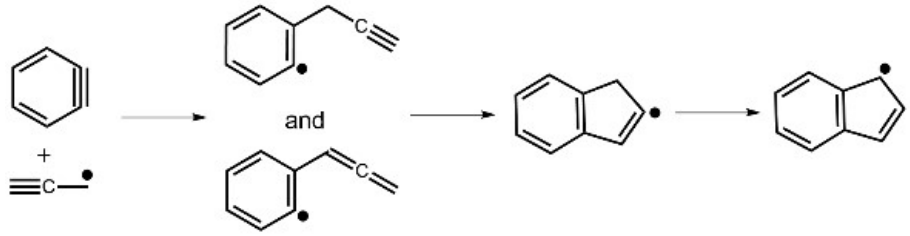

Scheme 2. Reaction path for *o*-benzyne + C_3H_3

mass-selected threshold photoelectron spectroscopy (ms-TPES), which is a unique tool for product detection and isomer-specific identification in reactive environments [34], we experimentally verified indenyl to be the major product of this reaction.

2. Experimental Setup

The experimental setup has been described previously [35] and only a short description is given here. We used a resistively heated SiC microtubular reactor (1 mm ID, 35-40 mm long) at ca. 1150 K and 10-20 mbar to generate the reactants, *o*-C_6H_4 and C_3H_3, and to follow their reactions. Benzoyl chloride and propargyl bromide served as precursors for *o*-C_6H_4 and C_3H_3, respectively:

$$C_6H_5\text{-}C(=O)Cl \rightarrow C_6H_4 + CO + HCl \quad (R3)$$

$$C_3H_3Br \rightarrow C_3H_3 + Br \quad (R4)$$

The pyrolysis conditions were chosen to maximize production of propargyl and *o*-benzyne and, thus, to maximize bimolecular reactions. The most important parameters are the reactants' number densities that can be influenced via the diluent's flow rates, the temperature of the sample container and the pyrolysis temperature. The pyrolysis temperature was controlled by the heating power and a previously determined power-temperature calibration (based on a type-c thermocouple measurement on the outside wall of the reactor) was used as a temperature measurement. The results presented in this paper were recorded at a pyrolysis temperature of 1150 K, at which both precursors make the desired reactants efficiently. By flowing argon over the liquid precursors, propargyl bromide and benzoyl chloride were added to the gas stream according to their vapor pressures. The flows were varied independently to achieve the targeted optimal conversion, leading to a total gas-stream of 6 sccm with about 1% C_3H_3Br and 2% C_6H_5-C(=O)Cl. The inlet pressure was about 100 mbar and the fluid dynamics simulation as described in Ref. [36] can be used to simulate the pressure in the reactor.

The reaction mixture was expanded into high vacuum to form an effusive molecular beam and was analyzed using the CRF-PEPICO spectrometer that combines a time-of-flight mass spectrometer and a velocity map imaging photoelectron spectrometer [37]. Ions and electrons were collected in delayed coincidence, permitting to record photoion mass-selected threshold photoelectron spectra (ms-TPES) [38].

These spectra were recorded at the vacuum-ultraviolet (VUV) beamline of the Swiss Light Source (SLS) at the Paul Scherrer Institute (PSI). A detailed description of the beamline is given in Ref. [39]. In short, synchrotron radiation was provided by a bending magnet, collimated and diffracted by a plane grating (150 grooves·mm^{-1}) with a resolving power of 1500. Higher harmonic radiation was suppressed in a rare gas filter operated with an Ar/Ne/Kr mixture at a pressure of 10 mbar. The photon energy was scanned in 10 meV steps and calibrated using autoionization resonances in Ar. For the analysis, threshold electrons were selected with an energy resolution of 5-7 meV and contributions of hot background electrons and false coincidences were subtracted [40, 41].

3. Results and Discussions

3.1 Overview mass spectrum

In a first step, we recorded photoionization mass spectra to ensure that the reactants, *o*-benzyne and propargyl, are formed cleanly in the flash pyrolysis source and that the targeted product, C_9H_7, is not a product formed in the pyrolysis of their respective precursors. To this end, Fig. 1 shows the sample mass spectra after flash pyrolysis of (a) benzoyl chloride and (b) propargyl bromide. The photon energies used here to acquire the overview mass spectra are chosen to be above the ionization energies of the targeted species, while trying to avoid, or at least, minimize dissociative photoionization. At a photon energy of 9.15 eV, the mass spectrum identifies C_6H_4, C_3H_3, C_5H_5, and the $C_6H_5{}^{35/37}Cl$ as intermediates and products in the flash photolysis of benzoyl chloride. The signal at *m/z* = 40 corresponds to naturally abundant ^{13}C isotopologues of the C_3H_3 radical. At a higher photon energy range of 9.8 eV (see Supplementary Material, Fig. S1), the C_6H_5CO and the precursor become visible as well. Most

importantly, the photon energies of 9.15 and 9.8 eV are above the ionization energy of the indene and respective indenyl radical, and therefore, the missing C_9H_7 peak indicates that C_9H_7 is not formed during the benzoyl chloride pyrolysis. The mass spectrum shown in Fig. 1(b), recorded at 9.0 eV, indicates that C_9H_7 is also not a product (or intermediate) of the flash pyrolysis of propargyl bromide. A second mass spectrum, recorded at 10.5 eV is shown in the Supplementary Material (Fig. S1).

We are therefore confident that any observed C_9H_7 product in the targeted C_6H_4 + C_3H_3 reaction is a product of this cross reaction.

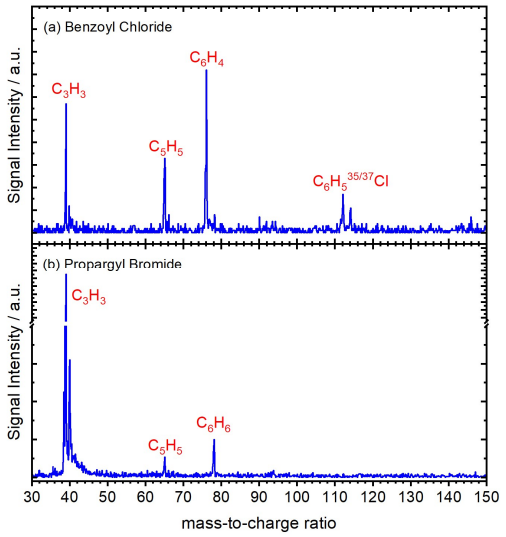

Fig. 1. (a) The experimentally observed mass spectra after flash pyrolysis of (a) benzoyl chloride and (b) propargyl bromide. The spectra were recorded at 9.15 and 9.0 eV, respectively, at a temperature of ~1150 K and a pressure of ~20 Torr. The absence of C_9H_7 signal in these control experiments provides evidence for the observed C_9H_7 to result from the cross reaction of *o*-benzyne with propargyl.

In a second step, we recorded photoionization mass spectra to ensure that C_9H_7 is produced in the *o*-C_6H_4 + C_3H_3 cross reaction in detectable amounts. A typical mass spectrum of the sampled gases from the outlet of the microtubular flash pyrolysis reactor is shown in Fig. 2. The mass spectrum was recorded at a photon energy of 9.2 eV and at a temperature of 1150 K. The targeted reactants appear in the mass spectra at m/z = 39 (C_3H_3) and 76 (C_6H_4), and as shown in Fig. 2, the anticipated product of the *o*-benzyne + propargyl reaction (R1) is detectable at m/z = 115 (C_9H_7). A cleaner mass spectrum, composed of individual spectra recorded at 8.1, 8.7, and 9.2 eV is shown in the Supplementary Material (Fig. S2). That mass spectrum is composed of different mass ranges recorded at different photon energies, thus suppressing peaks of precursors while highlighting the reactants and products.

While the focus of this work is on the C_9H_7 signal, it is important to understand how the precursors react and what other products are formed in the reactor as well. In addition to the C_3H_3, C_6H_4, and C_9H_7 species, the mass spectrum contains peaks at m/z = 78 (C_6H_6) and 152 ($C_{12}H_8$). As the latter peaks can be formed through C_3H_3 and C_6H_4 self-recombination reactions,

$$C_3H_3 + C_3H_3 \rightleftarrows C_6H_6 \quad \text{(R5)}$$

$$C_6H_4 + C_6H_4 \rightleftarrows C_{12}H_8 \quad \text{(R6)}$$

the presence of those peaks hints at the identity of the m/z = 39 (C_3H_3) and the m/z = 76 (C_6H_4) peaks as propargyl and *o*-benzyne, respectively. A more detailed description of the isomeric composition of the m/z = 78 peak will be provided in a future paper. A more rigorous identification of C_3H_3 and C_6H_4 based on the unique photoionization efficiency curves and threshold photoelectron spectra is given in the next section.

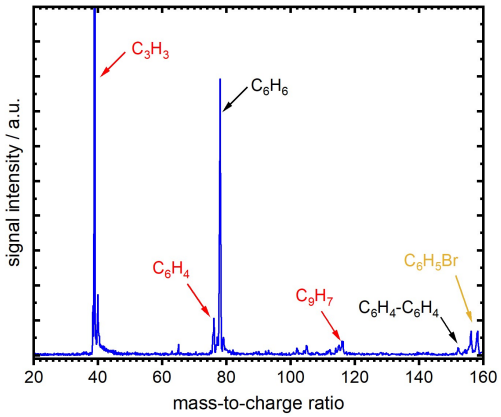

Fig. 2. Mass spectrum of the species exiting the microtubular reactor. The reactants (C_3H_3 and *o*-C_6H_4) and the product (C_9H_7) are marked. Also highlighted are C_6H_6 and C_6H_4-C_6H_4 from the propargyl + propargyl (R5) and *o*-benzyne + *o*-benzyne self-reactions (R6), respectively. C_6H_5Br is a product of the phenyl + Br reactions.

The peaks at m/z = 156 and 158 can be assigned to the ^{79}Br and ^{81}Br isotopologues of C_6H_5Br that results from the reaction of phenyl radicals (from the propargyl + propargyl reaction (R5)) with Br atoms that are a byproduct of the propargyl formation through flash pyrolysis of the propargyl bromide (R4). Accordingly, the peaks at m/z = 112 and 114 can be assigned to the ^{35}Cl and ^{37}Cl isotopologues of C_6H_5Cl. The corresponding photoionization efficiency curves for C_6H_5Br and C_6H_5Cl are summarized in the Supplementary Material (Fig. S3). The peaks at m/z = 65, 102, and 105 correspond to C_5H_5 and C_8H_6 side

products (most likely cyclopentadienyl and phenylacetylene) and a C_7H_5O intermediate.

3.2 *Identity of reactants*

In a third step, we confirmed the identity of the *m/z* = 39 (C_3H_3) and *m/z* = 76 (C_6H_4) reactants by photoion mass-selected threshold photoelectron spectra and photoion efficiency (PIE) curves, which together provide an isomer-selective fingerprint to assign molecular structures to the *m/z* peaks.

Figures 3 (a) and (b) show the PIE curve and the threshold photoelectron spectrum of the sampled *m/z* = 39 signal as a function of the photon energy in the range of 8.4-9.0 eV. The well-known characteristic PIE curve and ms-TPE spectrum of the propargyl radical are included for comparison [42, 43]. As can be seen, the experimentally observed PIE curve and ms-TPE spectrum agree exceptionally well with the literature references. The onset of the ion counts and the sharp resonance in the threshold photoelectron spectrum at 8.68 V is consistent with the adiabatic ionization energy of propargyl of 8.674 eV [43].

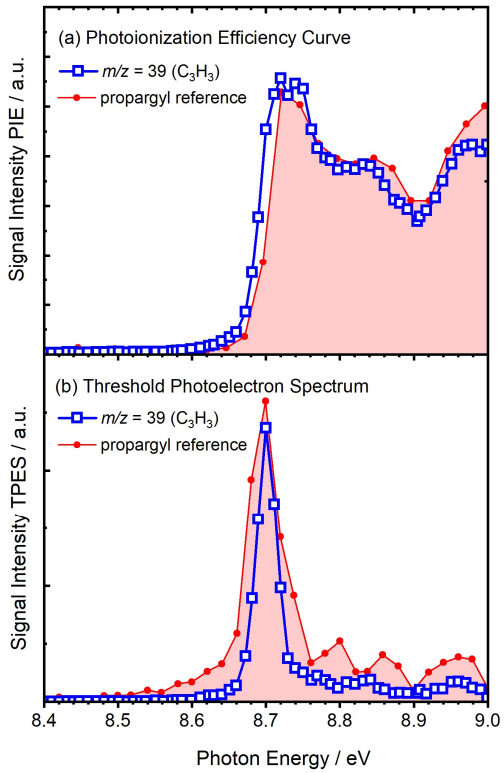

Fig. 3. (a) The experimentally observed photoionization efficiency curve (blue squares) and (b) the threshold photoelectron spectrum of *m/z* = 39 (blue squares) is compared to the propargyl (C_3H_3) references (red circles) as a function of photon energy. The spectra clearly identify the reactants as the propargyl (C_3H_3).

The data thus confirms that propargyl bromide decomposes according to reaction (R4) and that *m/z* = 39 can be unambiguously identified as the propargyl radical.

While propargyl bromide pyrolysis has been established to be a clean source of propargyl radicals, the development of a clean source for *o*-benzyne is more challenging. As described above, we used flash pyrolysis of benzoyl chloride as a source for *o*-benzyne as suggested by Zhang *et al.* [44].

The mass-selected threshold photoelectron spectrum of *m/z* = 76 is shown in Fig. 4. For the identification of the isomers, we had to cover a much broader photon energy range, and therefore, the energy steps were chosen to be coarser than for the data shown for *m/z* = 39. Here, we scanned from 9 to 9.8 eV and were able to identify two different isomers. Based on the literature, the feature near 9.0 eV can be assigned to the linear 1,5-hexadiyne-3-ene (HC≡C-CH=CH-C≡CH) isomer [45], while the feature near 9.6 eV is from *o*-benzyne contributions [46, 47]. The apparent feature at 9.3 eV is probably an artifact of the low spectral resolution, but contributions from a third isomer cannot be entirely ruled out.

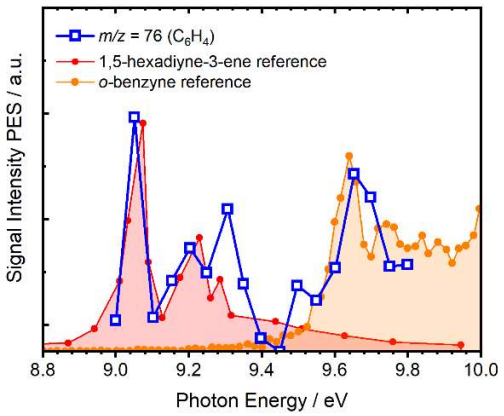

Fig. 4. The experimental mass-selected threshold photoelectron spectrum of *m/z* = 76 (blue squares) is compared to the 1,5-hexadiyne-3-ene and o-benzyne references (red circles) as a function of photon energy. The spectra clearly identify the reactants as both, the 1,5-hexadiyne-3-ene and *o*-benzyne isomers.

Using benzoyl chloride as a precursor for *o*-benzyne according to reaction (R3), we were not able to find conditions that would allow exclusive formation for *o*-benzyne and simultaneous formation of propargyl radicals under the same conditions. However, the reaction (R1) of *o*-benzyne with propargyl is barrierless [20], while a potential side reaction of the linear C_6H_4 isomer, 1,5-hexadiyne-3-ene, with propargyl would need to occur through a barrier that is typical for molecule-radical reactions [48], i.e., about 5-20 kcal/mol. Therefore, these molecule-radical reactions are much slower than the

barrierless reaction R1 and can be neglected in the further analysis.

3.3 *Isomer-selective product identification*

With the detection of a radical species with a molecular formula of C_9H_7 (m/z = 115), we are shifting our focus to the elucidation of its structural isomers. Given the mass spectra in Figs. 1 and 2, the possibilities of C_9H_7 coming from dissociative ionization or fragmentation can be ruled out. This leads us to conclude that C_9H_7 is a direct product of the *o*-benzyne + propargyl reaction (R1). In this final step, we use the photoionization efficiency curves and threshold photoelectron spectra to identify the indenyl radical as the predominant product of reaction (R1).

The mass-selective photoionization efficiency curve and threshold photoelectron spectrum for m/z = 115 (C_9H_7) are shown as a function of photon energy in Fig. 5 (a) and (b), respectively. They are combined with literature references for the indenyl radical [29]. For this, we scanned the photon energy from 7.2 to 7.65 eV to detect the characteristic features in the photoionization efficiency and in the photoelectron spectrum of the indenyl radical near 7.52 eV [49, 50], the known ionization energy of the indenyl radical. The observed features perfectly match the observed literature data, and we can comfortably identify the m/z = 115 (C_9H_7) signals as the indenyl radical. The PIE curve is not shown below 7.35 eV because it is contaminated with contributions from signal originating from ionization with higher harmonics of the VUV photons.

Additional methods to make the indenyl radical include the reaction of phenyl + propargyl as described in Ref. [18]. However, this reaction would proceed via the aliphatically substituted C_9H_8 isomers, leading likely also to phenyl-substituted propargyl radicals. These C_9H_7 isomers have also been calculated by Matsugi and Miyoshi as minima along the reaction path of reaction (R1). The photoelectron spectra for these two isomers 1-phenylpropargyl (C_6H_5-CHCCH) and 3-phenylpropargyl (C_6H_5-$CCCH_2$) are known: The ionization energies are 7.24 and 7.25 eV, respectively with ms-TPE spectra expanding above 7.4 eV [49, 50]. The isomers` spectra are included in Fig. 5.

The experimentally observed threshold photoelectron spectrum shows an apparent increase in signal intensities above 7.2 eV. However, the signal is too weak to show any features around 7.2 – 7.3 eV that are characteristic of phenyl substituted propargyl radicals. Thus, contributions of these two isomers cannot entirely be ruled out, but probably neglected. The non-resonantly stabilized cyclopentenyl-fused benzene structure (see Scheme 2) is unlikely to accumulate in large concentrations and is therefore not further considered in our analysis.

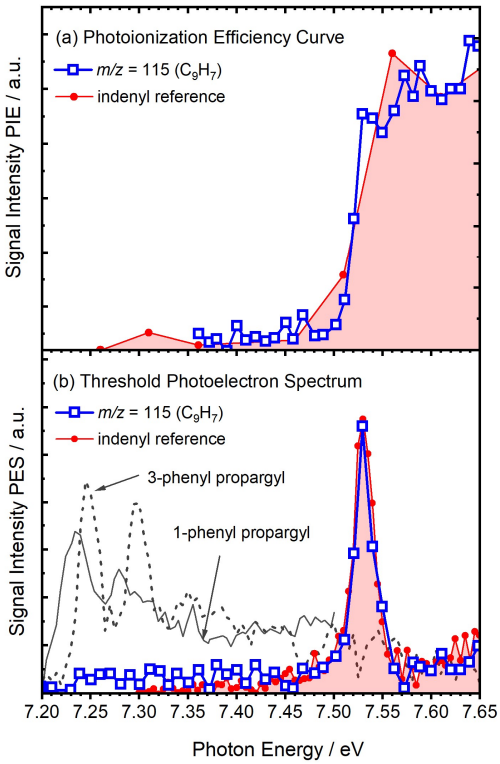

Fig. 5. (a) Experimentally observed photoion spectrum (blue squares) and (b) threshold photoelectron spectrum (blue squares) for m/z = 115 (C_9H_7) as a function of photon energy. Literature reference data is shown in red. The ms-TPE spectra of 1-phenyl propargyl and 3-phenyl propargyl from Ref. [50] are added.

The detection of indenyl as the predominant product of the *o*-C_6H_4 + C_3H_3 reaction (R1) agrees with the earlier theoretical work. Matsugi and Miyoshi calculated the transition energy to convert the C_6H_4-CH_2-CCH and C_6H_4-$CHCCH_2$ to the phenyl-substituted propargyl radicals to be about 165 kJ/mol^{-1}, compared to 70-80 kJ/mol^{-1} for the transition to form the cyclopentenyl-fused benzene ring that subsequently isomerizes to indenyl. Given the large differences in the energy of the transition states, it is not surprising that the phenyl-substituted propargyl radicals are not detected in our experiments. According to Matsugi and Miyoshi's work, all transition states are submerged to the *o*-benzyne + propargyl entrance channel. The rate constants for reaction (R1) were calculated by Matsugi and Miyoshi for a total pressure of 1 atm (N_2). They calculated the formation of the indenyl radical at 1200 K to be an order of magnitude faster than the formation of the phenyl-substituted propargyl radicals. The phenyl-substituted propargyl radicals are unlikely to be formed due to the high barriers for H migration following the initial association step. These results are consistent with previous work on the

reactions of phenyl with propargyl and cyclopentadienyl radicals, which also noted well-skipping at low pressures [18, 19].

The temperatures of our experiments were too low to observe the predicted dissociation into the resonantly stabilized fulvenallenyl (C_7H_5) radical + C_2H_2, which is predicted to become the dominant reaction channel near 2000 K (at atmospheric pressure). At our experimental conditions, no signal was detected at m/z = 89 (C_7H_5).

Conclusions

The work presented here explores the formation of a five-membered ring structure through the reaction of *o*-benzyne with propargyl. Such five-membered rings are essential to form curved and bowl-shaped polycyclic aromatic hydrocarbons (PAHs). Specifically, we studied the formation of the prototypical indenyl radical through the *o*-benzyne + propargyl reaction. To this end, we combined flash pyrolysis in a microtubular reactor to produce *o*-benzyne and propargyl radicals in significant concentrations to be able to detect the indenyl radical as the sole reaction product using photoion efficiency curves and threshold photoelectron spectroscopy, which were measured in coincidence using the CRF-PEPICO endstation at the Swiss Light Source of the Paul Scherrer Institute.

This work was motivated by the need to fully understand the impact of *o*-benzyne chemistry on molecular-weight growth processes and by the theoretical work of Matsugi and Miyoshi, who had calculated the potential energy surface and kinetics, which was waiting for an experimental confirmation. Our experimental observation agrees with the theoretical predictions.

o-Benzyne plays a unique role in PAH formation chemistry because of its biradical character, which provides a versatile route for five-membered rings annulated to benzene [35]. For example, the reaction studied here, *o*-benzyne with the propargyl radical, is barrierless and creates an intermediate with a radical site on the aromatic ring, which then allows for a rapid ring closure to yield these five-membered rings. Consequently, the indenyl radical has been identified as a predominant product of the *o*-benzyne + propargyl reaction. Kinetic modeling will need to be carried out to determine the reaction's importance and significance in combustion environments.

Declaration of competing interest

The authors declare that they have no known competing financial interests or personal relationships that could have appeared to influence the work reported in this paper.

Acknowledgements

N.H. is supported by the Gas-Phase Chemical Physics program of the US Department of Energy, Office of Science, Office of Basic Energy Science, Division of Chemical Sciences, Geosciences and Biosciences. He was also supported by the Helmholtz Association through a Helmholtz International Fellow Award. Sandia National Laboratories is a multimission laboratory managed and operated by National Technology and Engineering Solutions of Sandia, LLC, a wholly owned subsidiary of Honeywell International, Inc., for the U.S. DOE's National Nuclear Security Administration under contract DENA0003525. This paper describes objective technical results and analysis. Any subjective views or opinions that might be expressed in the paper do not necessarily represent the views of the U.S. DOE or the U.S. Government. The experiments were performed at the VUV (x04db) beamline of the Swiss Light Source (SLS) located at Paul Scherrer Institute (PSI), Villigen, Switzerland. The authors are grateful to Hannes Lüdtke and Patrick Ascher for supporting the measurement campaign.

Supplementary material

Supplementary material is provided.

References

[1] H. Wang, Formation of nascent soot and other condensed-phase materials in flames, Proc. Combust. Inst., 33 (2011), 41-67.

[2] H. Bockhorn, A. D'Anna, A.F. Sarofim, and H. Wang, eds. *Combustion generated fine carbonaceous particles*. 2014, KIT Scientific publishing.

[3] Y. Wang and S.H. Chung, Soot formation in laminar counterflow flames, Progr. Energy Combust. Sci., 74 (2019), 152-238.

[4] R.I. Kaiser and N. Hansen, An aromatic universe – A physical chemistry perspective, J. Phys. Chem. A, 125 (2021), 3826-3840.

[5] J.W. Martin, M. Salamanca, and M. Kraft, Soot inception: Carbonaceous nanoparticle formation in flames, Progr. Energy Combust. Sci., 88 (2022), 100956.

[6] R. Teoh, U. Schumann, C. Voigt, T. Schripp, M. Shapiro, Z. Engberg, J. Molloy, G. Koudis, and M.E. Stettler, Targeted use of sustainable aviation fuel to maximize climate benefits, Environ. Sci. Techn., 56 (2022), 17246-17255.

[7] D.S. Lee, D.W. Fahey, A. Skowron, M.R. Allen, U. Burkhardt, Q. Chen, S.J. Doherty, S. Freeman, P.M. Forster, and J. Fuglestvedt, The contribution of global aviation to anthropogenic climate forcing for 2000 to 2018, Atmos. Environ., 244 (2021), 117834.

[8] T. Schripp, B.E. Anderson, U. Bauder, B. Rauch, J.C. Corbin, G.J. Smallwood, P. Lobo, E.C. Crosbie, M.A. Shook, and R.C. Miake-Lye, Aircraft engine particulate matter emissions from sustainable aviation fuels: Results from ground-based measurements during

the NASA/DLR campaign ECLIF2/ND-MAX, Fuel, 325 (2022), 124764.
[9] P. Oßwald, J. Zinsmeister, T. Kathrotia, M. Alves-Fortunato, V. Burger, R. van Der Westhuizen, C. Viljoen, K. Lehto, R. Sallinen, and K. Sandberg, Combustion kinetics of alternative jet fuels, Part-I: Experimental flow reactor study, Fuel, 302 (2021), 120735.
[10] T. Schripp, B. Anderson, E.C. Crosbie, R.H. Moore, F. Herrmann, P. Oßwald, C. Wahl, M. Kapernaum, M. Köhler, and P. Le Clercq, Impact of alternative jet fuels on engine exhaust composition during the 2015 ECLIF ground-based measurements campaign, Environ. Sci. Techn., 52 (2018), 4969-4978.
[11] N. Hansen, B. Yang, M. Braun-Unkhoff, A. Ramirez, and G. Kukkadapu, Molecular-growth pathways in premixed flames of benzene and toluene doped with propyne, Combust. Flame, 243 (2022), 112075.
[12] V. Kislov and A. Mebel, Ab initio G3-type/statistical theory study of the formation of indene in combustion flames. I. Pathways involving benzene and phenyl radical, J. Phys. Chem. A, 111 (2007), 3922-3931.
[13] A.M. Mebel, Y. Georgievskii, A.W. Jasper, and S.J. Klippenstein, Pressure-dependent rate constants for PAH growth: formation of indene and its conversion to naphthalene, Faraday Disc., 195 (2016), 637-670.
[14] A.M. Mebel, A. Landera, and R.I. Kaiser, Formation mechanisms of naphthalene and indene: from the interstellar medium to combustion flames, J. Phys. Chem. A, 121 (2017), 901-926.
[15] A.N. Morozov and A.M. Mebel, Theoretical study of the reaction mechanism and kinetics of the phenyl+ propargyl association, Phys. Chem. Chem. Phys., 22 (2020), 6868-6880.
[16] G. da Silva and J.W. Bozzelli, Indene formation from alkylated aromatics: kinetics and products of the fulvenallene+acetylene reaction, J. Phys. Chem. A, 113 (2009), 8971-8978.
[17] B. Shukla, A. Susa, A. Miyoshi, and M. Koshi, Role of phenyl radicals in the growth of polycyclic aromatic hydrocarbons, J. Phys. Chem. A, 112 (2008), 2362-2369.
[18] D.E. Couch, G. Kukkadapu, A.J. Zhang, A.W. Jasper, C.A. Taatjes, and N. Hansen, The role of radical-radical chain-propagating pathways in the phenyl + propargyl reaction, Proc. Combust. Inst., 39 (2023), 643-651.
[19] D.E. Couch, A.W. Jasper, G. Kukkadapu, M.M. San Marchi, A.J. Zhang, C.A. Taatjes, and N. Hansen, Molecular-weight growth by the phenyl+cyclopentadienyl reaction: Well-skipping and ring-opening, Combust. Flame, 257 (2023), 112439.
[20] A. Matsugi and A. Miyoshi, Reactions of o-benzyne with propargyl and benzyl radicals: potential sources of polycyclic aromatic hydrocarbons in combustion, Phys. Chem. Chem. Phys., 14 (2012), 9722-9728.
[21] C. Wentrup, The benzyne story, Austr. J. Chem., 63 (2010), 979-986.
[22] H.H. Wenk, M. Winkler, and W. Sander, One century of aryne chemistry, Angew. Chem. Int. Ed., 42 (2003), 502-528.
[23] A. Matsugi, Thermal decomposition of benzyl radicals: kinetics and spectroscopy in a shock tube, J. Phys. Chem. A, 124 (2020), 824-835.
[24] A. Comandini, S. Abid, and N. Chaumeix, Polycyclic aromatic hydrocarbon growth by diradical cycloaddition/fragmentation, J. Phys. Chem. A, 121 (2017), 5921-5931.
[25] A. Comandini and K. Brezinsky, Theoretical study of the formation of naphthalene from the radical/π-bond addition between single-ring aromatic hydrocarbons, J. Phys. Chem. A, 115 (2011), 5547-5559.
[26] B. Shukla, K. Tsuchiya, and M. Koshi, Novel products from C6H5+C6H6/C6H5 reactions, J. Phys. Chem. A, 115 (2011), 5284-5293.
[27] L. Monluc, A.A. Nikolayev, I.A. Medvedkov, V.N. Azyazov, A.N. Morozov, and A.M. Mebel, The reaction of o-benzyne with vinylacetylene: An unexplored way to produce naphthalene, ChemPhysChem, 23 (2022), e202100758.
[28] K.O. Johansson, M.P. Head-Gordon, P.E. Schrader, K.R. Wilson, and H.A. Michelsen, Resonance-stabilized hydrocarbon-radical chain reactions may explain soot inception and growth, Science, 361 (2018), 997-1000.
[29] M.N. McCabe, P. Hemberger, E. Reusch, A. Bodi, and J. Bouwman, Off the beaten path: Almost clean formation of indene from the ortho-benzyne + allyl reaction, J. Phys. Chem. Lett., 11 (2020), 2859-2863.
[30] A. Comandini and K. Brezinsky, Radical/π-bond addition between o-benzyne and cyclic C5 hydrocarbons, J. Phys. Chem. A, 116 (2012), 1183-1190.
[31] W. Li, J. Yang, L. Zhao, D. Couch, M.S. Marchi, N. Hansen, A.N. Morozov, A.M. Mebel, and R.I. Kaiser, Gas-phase preparation of azulene (C10H8) and naphthalene (C10H8) via the reaction of the resonantly stabilized fulvenallenyl (C7H5˙) and propargyl (C3H3˙) radicals, Chem. Sci., 14 (2023), 9795-9805.
[32] D.E. Couch, A.J. Zhang, C.A. Taatjes, and N. Hansen, Experimental observation of hydrocarbon growth by resonance-stabilized radical–radical chain reaction, Angew. Chem. Int. Ed., 60 (2021), 27230-27235.
[33] G. Kukkadapu, S. Wagnon, W. Pitz, and N. Hansen, Identification of the molecular-weight growth reaction network in counterflow flames of the C3H4 isomers allene and propyne, Proc. Combust. Inst., 38 (2021), 1477-1485.
[34] P. Hemberger, A. Bodi, T. Bierkandt, M. Köhler, D. Kaczmarek, and T. Kasper, Photoelectron photoion coincidence spectroscopy provides mechanistic insights in fuel synthesis and conversion, Energy Fuels, 35 (2021), 16265-16302.
[35] M.N. McCabe, P. Hemberger, D. Campisi, J.C. Broxterman, E. Reusch, A. Bodi, and J. Bouwman, Formation of phenylacetylene and benzocyclobutadiene in the ortho-benzyne+ acetylene reaction, Phys. Chem. Chem. Phys., 24 (2022), 1869-1876.
[36] Q. Guan, K.N. Urness, T.K. Ormond, D.E. David, G.B. Ellison, and J.W. Daily, The properties of a micro-reactor for the study of the unimolecular decomposition of large molecules, Int. Rev. Phys. Chem., 33 (2014), 447-487.
[37] B. Sztáray, K. Voronova, K.G. Torma, K.J. Covert, A. Bodi, P. Hemberger, T. Gerber, and D.L. Osborn, CRF-PEPICO: Double velocity map imaging photoelectron photoion coincidence spectroscopy for reaction kinetics studies, J. Chem. Phys., 147 (2017).
[38] T. Baer and R.P. Tuckett, Advances in threshold photoelectron spectroscopy (TPES) and threshold

photoelectron photoion coincidence (TPEPICO), Phys. Chem. Chem. Phys., 19 (2017), 9698-9723.
[39] M. Johnson, A. Bodi, L. Schulz, and T. Gerber, Vacuum ultraviolet beamline at the Swiss Light Source for chemical dynamics studies, Nuclear Inst. and Methods in Physics Research, , 610 (2009), 597-603.
[40] A. Bodi, B. Sztáray, T. Baer, M. Johnson, and T. Gerber, Data acquisition schemes for continuous two-particle time-of-flight coincidence experiments, Rev. Sci. Instr., 78 (2007), 084102.
[41] B. Sztáray and T. Baer, Suppression of hot electrons in threshold photoelectron photoion coincidence spectroscopy using velocity focusing optics, Rev. Sci. Instr., 74 (2003), 3763-3768.
[42] P. Hemberger, M. Lang, B. Noller, I. Fischer, C. Alcaraz, B.K. Cunha de Miranda, G.A. Garcia, and H. Soldi-Lose, Photoionization of propargyl and bromopropargyl radicals: A threshold photoelectron spectroscopic study, J. Phys. Chem. A, 115 (2011), 2225-2230.
[43] T. Zhang, X.N. Tang, K.-C. Lau, C.Y. Ng, C. Nicolas, D.S. Peterka, M. Ahmed, M.L. Morton, B. Ruscic, R. Yang, L.X. Wei, C.Q. Huang, B. Yang, J. Wang, L.S. Sheng, Y.W. Zhang, and F. Qi, Direct identification of propargyl radical in combustion flames by vacuum ultraviolet photoionization mass spectrometry, J. Chem. Phys., 124 (2006), 074302.
[44] X. Zhang, V.M. Bierbaum, G.B. Ellison, and S. Kato, Gas-phase reactions of organic radicals and diradicals with ions, J. Chem. Phys., 120 (2004), 3531-3534.
[45] F. Brogli, E. Heilbronner, J. Wirz, E. Kloster-Jensen, R.G. Bergman, K.P.C. Vollhardt, and A.J. Ashe III, The consequences of σ and π conjugative interactions in mono-, di- and triacetylenes. A photoelectron spectroscopic investigation, Helv. Chim. Acta, 58 (1975), 2620-2645.
[46] D. Kaiser, E. Reusch, P. Hemberger, A. Bodi, E. Welz, B. Engels, and I. Fischer, The ortho-benzyne cation is not planar, Phys. Chem. Chem. Phys., 20 (2018), 3988-3996.
[47] Z. Pan, A. Bodi, J.A. van Bokhoven, and P. Hemberger, On the absolute photoionization cross section and threshold photoelectron spectrum of two reactive ketenes in lignin valorization: fulvenone and 2-carbonyl cyclohexadienone, Phys. Chem. Chem. Phys., 24 (2022), 3655-3663.
[48] J. Bouwman, A. Bodi, J. Oomens, and P. Hemberger, On the formation of cyclopentadiene in the C3H5 + C2H2 reaction, Phys. Chem. Chem. Phys., 17 (2015), 20508-20514.
[49] P. Hemberger, M. Steinbauer, M. Schneider, I. Fischer, M. Johnson, A. Bodi, and T. Gerber, Photoionization of rhree isomers of the C9H7 radical, J. Phys. Chem. A, 114 (2010), 4698-4703.
[50] F. Holzmeier, M. Lang, P. Hemberger, and I. Fischer, Improved ionization energies for the two isomers of phenylpropargyl radical, ChemPhysChem, 15 (2014), 3489-3492.